One-Dimensional Random Lasing in a Single Organic Nanofiber

Francesco Quochi,* Fabrizio Cordella, Andrea Mura, and Giovanni Bongiovanni

Dipartimento di Fisica, Università di Cagliari, I-09042 Monserrato (CA), Italy

Frank Balzer

Institut für Physik/ASP, Humboldt-Universität zu Berlin, Newtonstrasse 15, D-12489 Berlin, Germany

Horst-Günter Rubahn

Fysisk Institut, Syddansk Universitet, Campusvej 55, DK-5230 Odense M, Denmark

One-dimensional light amplification in individual *p*-sexiphenyl nanofibers is investigated. The influence of fiber morphology on light propagation properties is studied via optical and atomic force microscopy. Isolated nanofibers are shown to yield low-threshold random laser emission in the deep blue. Model calculations of coherent light propagation in one-dimensional random media qualitatively reproduce the experimental results. Implications for photonic nanosensors are briefly discussed.

Introduction

The past decade has witnessed great advancement in the field of organic thin layers based on small oligomers such as thiophenes and phenylenes. Conjugated organic molecules are often insoluble in common solvents and have to be deposited on substrates by vacuum sublimation techniques, e.g., molecular-beam epitaxy[1] and hot-wall epitaxy.[2] When deposition of *p*-sexiphenyl (*p*-6P) and other conjugated oligomers occurs on substrates exhibiting large surface electric dipoles, dipole−induced dipole interaction can lead to the self-assembly of molecular aggregates with submicrometric cross-sectional dimensions, truly macroscopic lengths (up to 1 mm), and a high degree of crystallinity.[2−4] Depending on the substrate type and preparation procedure, linear and ring-shape aggregates (usually referred to as nanofibers and microrings) are formed.[5] Such nanoaggregates have been shown to yield efficient and aniso-tropic blue luminescence,[6] optical wave-guiding,[7] optical up-conversion,[8] resonant Raman amplification,[9] and laserlike emission.[10] In addition to the optical properties, carrier mobilities ranging from 0.03 to 0.66 cm^2 V^{-1} s^{-1} have been achieved in organic nanofibers.[11,12] Therefore, self-assembled molecular nanoaggregates have been inferred to have great potential for next-generation nanotechnologies such as nanoscale photonics and optoelectronics. Also, the photonic properties of molecular nanoaggregates could usher in novel sensing applications of organic nanofibers and microrings in the future.

Laserlike emission reported in early experiments in *p*-6P nanofibers grown on mica has been described in terms of random lasing.[10] Those early experiments relate to ensemble-averaged measurements on systems of close-packed nanofibers which do optically interact with one another. Random lasing in close-packed, interacting nanofibers might actually differ from lasing in one-dimensional (1-D) single nanofibers. To obtain deep knowledge about the intrinsic photonic and lasing response

of self-assembled *p*-6P nanofibers and its implications for photonic applications, it is therefore necessary to perform spectroscopy on single (linear) nanofibers.

In this paper, we investigate laser action in single *p*-6P nanofibers grown on (001)-oriented muscovite mica. This is done in a selection of samples exhibiting regions very sparse in nanofibers. We show that random lasing occurs in isolated nanofibers as a consequence of 1-D coherent optical feedback along the nanofibers' axis. This determination, inferred from the observed spatial correlation between the nanofibers' optical and morphological characteristics, is further supported by computer simulations of coherent propagation of light in 1-D random media. Implications of our results concern the applica-tion of organic nanofibers in nanotechnology, e.g., as active photonic nanosensors.

Experimental Details

Sheets of muscovite mica (SPI) are cleaved in air and are transferred immediately after cleavage into a high-vacuum apparatus (base pressure of 5×10^{-8} mbar). Before organic material is deposited, the samples are outgassed at a temperature of around 400 K such that low-energy electron diffraction shows the well-known hexagonal surface structure of clean mica with electric surface dipoles present. *p*-Sexiphenyl is deposited from a home-built Knudsen cell by vacuum sublimation; during the deposition the pressure inside the vacuum system rises to 2×10^{-7} mbar. Long *p*-6P needles grow for deposition rates of 0.1 Å/s and at substrate temperatures around 420 K.

Laser action is photoinduced using ultrashort (∼150 fs) laser pulses of a frequency-doubled (390 nm) Ti:sapphire regenerative amplifier running at a repetition frequency of 1 kHz. The UV beam is focused to a spot size with a diameter of ∼180 μm on the sample. The samples are excited at normal incidence from the back surface of the mica substrate; a polarization controller ensures that the pump field polarization is perpendicular to the axis of the nanofibers (lying on the front surface) for maximum optical absorption.[2] The nanofibers' emission is collected from

* To whom correspondence should be addressed. Phone: +39-070-6754843. Fax: +39-070-510171. E-mail: francesco.quochi@dsf.unica.it.
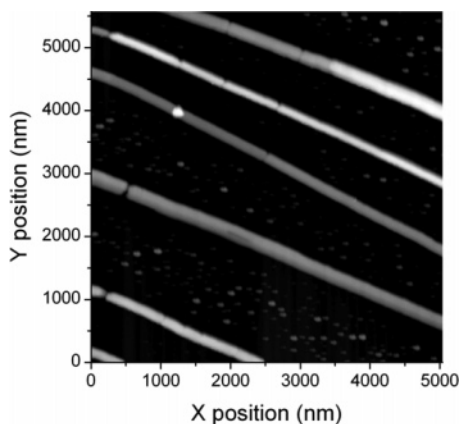
1-D Random Lasing in a Single Organic Nanofiber

J. Phys. Chem. B, Vol. 109, No. 46, 2005 **21691**

Figure 1. Gray-scale AFM topographic image of the surface morphology of *p*-6P nanofibers grown on muscovite mica. Black and white levels correspond to *p*-6P heights of 0 and 95 nm, respectively.

the front surface using a 32× microscope objective which focuses it onto the plane of the input slit of a single imaging spectrometer equipped with a liquid N_2 (LN_2) cooled charge-coupled device (CCD). Setting the spectrograph to zeroth-order diffraction and fully opening the input slit (operation in spatial mode), we are able to image a ∼65 (horizontal) × 200 (vertical) μm^2 area within the excitation spot, with a linear spatial resolution of about 2 μm. Tuning the spectrometer to first-order diffraction and closing the input slit to 100 μm (operation in spectral mode), we can resolve the emission of a single nanofiber aligned vertically (parallel to the input slit) with a spectral resolution of about 0.2 nm, while the vertical spatial resolution is still ∼2 μm. Complementary morphological characterization is carried out by scanning-probe atomic force microscopy (AFM) using Si probes in tapping mode in air.

Results and Discussion

Figure 1 depicts the surface morphology of a ∼5 × 5.5 μm^2 substrate area with sparse *p*-6P nanofibers. Epifluorescence measurements made in an optical microscope show that isolated nanofibers can actually be tens to several hundreds of micrometers long (not shown). The topographic image in Figure 1 displays typical features of isolated nanofibers on the length scale of a few micrometers. The nanofibers have a base width of 300 nm or larger, which enables wave-guiding of the deep-blue spontaneous emission of *p*-6P beyond 400 nm. The small islands lying between adjacent nanofibers are remnants of the nucleation process of *p*-6P into oriented fibers.[13] Occurrence of cracks, which are typically 50−300 nm wide, implies segmentation of the nanofibers. Such thin breaks occur possibly at the end of the material growth process as a result of a surface thermal gradient while the substrate is cooling[4] or are due to an instability similar to the case of functionalized organic nanofibers on mica.[14] Breaks characterize most nanofibers in most samples albeit there exist nearly break-free nanofibers. In addition to special sites where sudden variation in fiber width or height occurs (also evident in Figure 1), cracks are allegedly responsible for scattering and partial back-reflection of the optical mode(s) confined in the nanofibers; hence, they potentially contribute to the buildup of 1-D coherent optical feedback for lasing.

Random lasing from isolated nanofibers starts at pump fluences on the order of 10 $\mu J/cm^2$ per pulse. Lasing nanofibers are reported in Figure 2. Figure 2a shows a lasing micrograph taken in imaging mode slightly above threshold. It displays both lasing from vertically aligned nanofibers and spontaneous
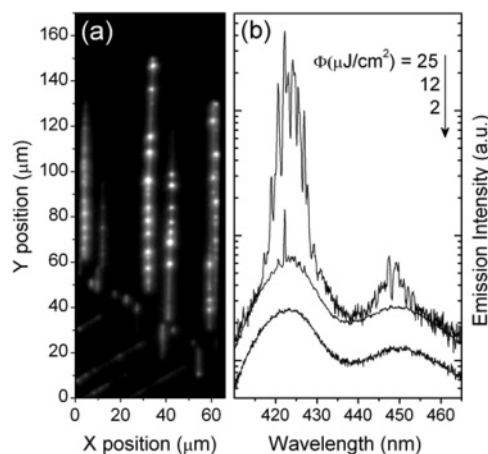

Figure 2. (a) Gray-scale optical emission intensity image of lasing and luminescent *p*-6P nanofibers excited at a pump fluence (ϕ) of 15 $\mu J/cm^2$ per pulse. The gray-level scale is logarithmic. The *y* coordinate refers to the position along the vertical direction, which is parallel to the input slit of the detection system. (b) Emission intensity spectra of the nanofiber positioned at $x \approx 30$ μm in panel a and extending vertically from $y \approx 50$ μm to $y \approx 150$ μm for different values of the pump fluence. Note that the threshold fluence is lower than 12 $\mu J/cm^2$ per pulse.

emission from a set of neighboring nanofibers oriented approximately at 60° with respect to the vertical axis of the detection system. The latter faintly appear in the lower part of the graph. Scattering of the lasing emission into out-of-plane directions does not take place homogeneously along the nanofibers' axis; conversely, scattering is highly spotted, indicating that wave-guiding is interleaved with light scattering and outcoupling at special sites along the fibers. Emission spectra relating to the ∼100 μm long nanofiber placed at the center of the imaging field of view in Figure 2a are reported in Figure 2b. They refer to the emission spatially integrated over the whole nanofiber length. Below threshold, spontaneous emission exhibits a broad vibronic progression with 0−1 and 0−2 emission bands peaked near 425 and 450 nm, respectively.

When the threshold fluence is reached, narrow peaks emerge from the spontaneous emission spectrum (0−1 band) and their number increases with increasing pump fluence. The lasing behavior, very similar to that reported in previous ensemble-averaged measurements carried out in systems of close-packed nanofibers, is attributed to *coherent* random lasing due to coherent (or amplitude) feedback.[15] The large *p*-6P gain bandwidth makes random lasing possible also at the 0−2 vibronic peak with only slightly higher threshold pump fluences. We notice that the spontaneous emission intensity sharply saturates for pump fluences larger than the threshold fluence, in agreement with basic laser theory for a single emitter such as a single nanofiber. By contrast, in ensemble-averaged experiments many excited nanofibers do not reach threshold; hence, they contribute to the system response only with spontaneous emission, and the total luminescence intensity does not clamp to its threshold level.[10]

Correlation between the lasing properties and the morphological characteristics of individual nanofibers allows us to gain insight into the origin of coherent optical feedback leading to random lasing in isolated nanofibers. All this is illustrated throughout the four panels of Figure 3. Panels a and b display a lasing micrograph of an isolated nanofiber and its intensity profile, respectively. By zooming in on a smaller fiber region, it turns out that scattering of the lasing emission guided by the nanofiber occurs at the fiber breaks. In fact, excellent cor-
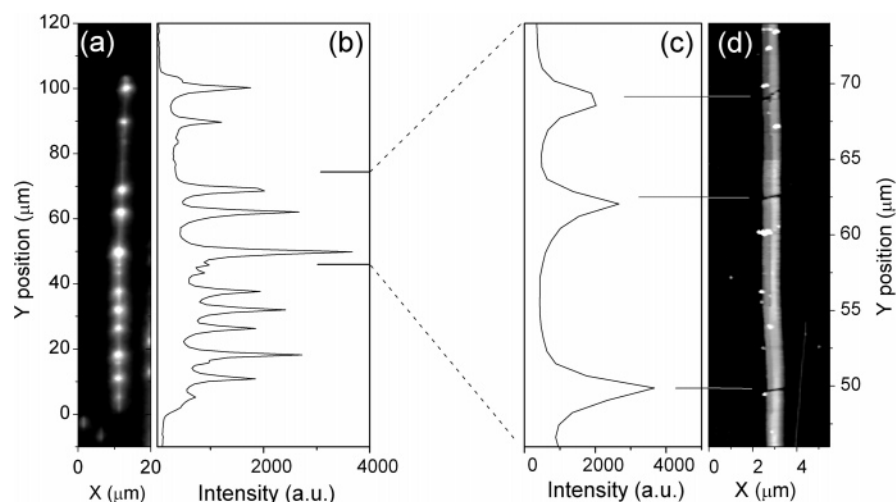
Figure 3. (a) Logarithmic gray-scale image of the lasing emission intensity of an isolated nanofiber. The pump fluence is 15 $\mu J/cm^2$ per pulse. (b) Spatial profile of the lasing emission intensity shown on a linear scale. (c) Lasing intensity profile zoomed in on the region delimited by the horizontal markers placed in panel b. (d) Gray-scale AFM topographic image zoomed in on the same region. Black and white levels correspond to p-6P heights of 0 and 95 nm, respectively. The horizontal markers show the correspondence between the positions of the bright lasing spots and those of the nanofiber breaks.

respondence is found between the positions of the lasing spots and those of the fiber breaks, as shown in panels c and d. Very similar results are obtained in other isolated nanofibers. Therefore, correlated lasing measurements and AFM measurements strongly support the idea that back-reflections of the wave-guided lasing mode(s) at the fiber break interfaces (where strong scattering occurs) are the main source of coherent optical feedback responsible for 1-D random lasing in isolated nanofibers.

The experimental results are further supported by computer simulations of random optical spectra in one-dimensional nanostructures such as our nanofibers. The theoretical model relates to the propagation of a coherent optical field of variable wavelength through a nanofiber using a standard transfer-matrix approach. Coherent propagation (with arbitrary material gain) accounts for transmission resonances which are the relevant channels for lasing;[16] thus, a coherent propagation model highlights all the spectral features of lasing. Calculations are done for a one-dimensional structure, neglecting cross-sectional (modal) effects. In the model structure, several material slabs, simulating fiber segments, are separated by thin air gaps, which in turn stand for fiber breaks. The refractive index step between the material ($n \approx 1.7$ for p-6P[7]) and air causes partial back-reflection of the (plane-wave) optical field at each material−air interface. Light scattering into directions other than the fiber axis at the break locations is introduced in the model in the form of linear extinction of the one-dimensionally propagating field through the air gaps. Other optical losses such as material reabsorption and waveguide scattering are compensated by gain. The total loss actually determines the spectral width of the coherent propagation modes. Simulations are carried out with the structural data (deduced from AFM) of the nanofiber shown in Figures 2 and 3, in terms of both material slab lengths and air gap widths. The intensity spectrum of the coherent field is calculated at specific break locations and compared to the lasing emission spectrum measured at the same locations (Figure 4). The theoretical spectra are in qualitative agreement with the experimental ones, from which we infer that the present model is able to describe the basics of lasing in a 1-D random system. In particular, the model reproduces the spectral density of the lasing modes and accounts for intensity variation of the peaks as a function of the position along the nanofiber. However,
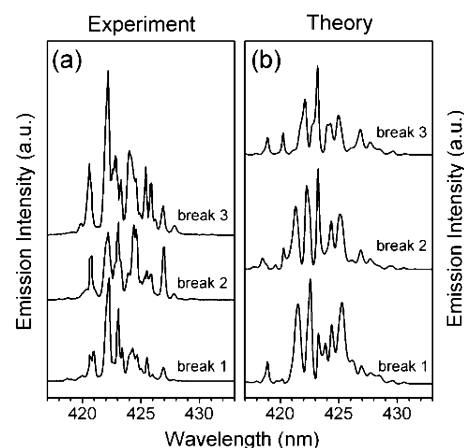

Figure 4. (a) Lasing emission spectra measured at the locations of the three nanofiber breaks shown in Figure 3. The pump fluence is 25 $\mu J/cm^2$ per pulse. (b) Optical intensity spectra calculated at the same fiber locations on the basis of a one-dimensional coherent propagation model using a transfer-matrix formalism. Calculation details are given in the text.

inclusion in the model of cross-sectional effects relating to the propagation of light in the actual nanofiber is necessary to predict the positions of the lines and their relative intensities. This goes beyond the scope of this paper. Experimentally, both the spectral and spatial patterns of the random modes are found to be highly reproducible over long time periods, so we infer that the nanofibers' material and morphology are robust against persistent laser irradiation at the pump levels used for the measurements.

The calculated intensity spectrum is very sensitive to changes in the refractive index as well as structural changes in the position and width of the fiber breaks, suggesting that self-assembled p-6P nanofibers have great potential for photonic sensing. For instance, surface adsorption of molecular species in nanofibers assembled from suitably functionalized oligomers[14] would generate photonic chemosensing, e.g., by modulation of the effective index of the nanofiber propagation modes. Furthermore, operation at the onset of random lasing should lead to increased sensitivity of nanofiber-based sensors.[17]

We add that the feasibility of advanced sensing applications (e.g., position sensors) based on self-assembled organic nano-

1-D Random Lasing in a Single Organic Nanofiber

J. Phys. Chem. B, Vol. 109, No. 46, 2005 **21693**

fibers stems from a number of capabilities, among which are (i) the ability of controlling the material aggregation process into highly crystalline nanostructures with suitable morphological characteristics, so as to achieve the desired photonic response, and (ii) the possibility of transferring large numbers of homogeneous nanofibers onto suitable substrates (such as ITO, Si, and SiO_2) for device realization, while ensuring high-density packing and a high degree of orientation. Concerning the transfer capability, encouraging results have already been obtained with self-assembled organic nanofibers from *p*-6P[18,19] and thiophene/*p*-phenylene co-oligomers.[20]

Conclusions

We studied 1-D random laser action in single *p*-6P nanofibers realized on mica via self-assembly. The interpretation of the experimental results, assisted by model calculations of propagation of coherent light in 1-D random media, suggests that organic nanofibers have potential for photonics and sensing applications at the nanoscale.

References and Notes

(1) Balzer, F.; Rubahn, H.-G. *Surf. Sci.* **2002**, *507−510*, 588.

(2) Andreev, A.; Matt, G.; Brabec, C. G.; Sitter, H.; Badt, D.; Seyringer, H.; Sariciftci, N. S. *Adv. Mater.* **2000**, *12*, 629.

(3) Yanagi, H.; Morikawa, T. *Appl. Phys. Lett.* **1999**, *75*, 187.

(4) Balzer, F.; Rubahn, H.-G. *Appl. Phys. Lett.* **2001**, *79*, 3860.

(5) Balzer, F.; Beermann, J.; Bozhevolnyi, S. I.; Simonsen, A. C.; Rubahn, H.-G. *Nano Lett.* **2003**, *3*, 1311.

(6) Yanagi, H.; Ohara, T.; Morikawa, T. *Adv. Mater.* **2001**, *13*, 1452.

(7) Balzer, F.; Bordo, V. G.; Simonsen, A. C., Rubahn, H.-G. *Phys. Rev. B* **2003**, *67*, 115408.

(8) Balzer, F.; K. Al Shamery, K., Neuendorf, R.; Rubahn, H.-G. *Chem. Phys. Lett.* **2003**, *368*, 307.

(9) Yanagi, H., Yoshiki, A. *Appl. Phys. Lett.* **2004**, *84*, 4783.

(10) Quochi, F.; Cordella, F.; Orrù, R.; Communal, J. E.; Verzeroli, P.; Mura, A., Bongiovanni, G.; Andreev, A.; Sitter, H.; Sariciftci, N. S. *Appl. Phys. Lett.* **2004**, *84*, 4454.

(11) Kjelstrup-Hansen, J.; Henrichsen, H. H.; Bøggild, P.; Rubahn, H.-G. *Thin Solid Films*, in press.

(12) Ichikawa, M.; Yanagi, H.; Shimizu, Y.; Hotta, S.; Suganuma, N.; Koyama, T.; Taniguchi, Y. *Adv. Mater.* **2002**, *14*, 1272.

(13) Plank, H., Resel, R.; Sitter, H.; Andreev, A.; Sariciftci, N. S.; Hlawacek, G.; Teichert, C.; Thierry, A.; Lotz, B. *Thin Solid Films* **2003**, *443*, 108.

(14) Schiek, M.; Lützen, A.; Koch, R.; Al-Shamery, K.; Balzer, F.; Frese, R.; Rubahn, H.-G. *Appl. Phys. Lett.* **2005**, *86*, 153107.

(15) Cao, H. *Waves Random Media* **2003**, *13*, R1 and references therein.

(16) Burin, A. L.; Ratner, M. A.; Cao, H.; Chang, S. H. *Phys. Rev. Lett.* **2002**, *88*, 093904.

(17) Aimée, R.; Zhu, Z.; Madigan, C. F.; Swager, T. M.; Buloviæ, V. *Nature* **2005**, *434*, 876.

(18) Brewer, J.; Rubahn, H.-G. *Phys. Status Solidi C*, in press.

(19) Brewer, J.; Maibohm, C.; Jozefowski, L.; Bagatolli, L.; Rubahn, H.-G. *Nanotechnology*, in press.

(20) Yanagi, H.; Morikawa, T.; Hotta, S. *Appl. Phys. Lett.* **2002**, *81*, 1512.